JOURNAL OF VIROLOGY, Oct. 2005, p. 13082–13093 Vol. 79, No. 20
0022-538X/05/$08.00+0 doi:10.1128/JVI.79.20.13082–13093.2005

Herpes Simplex Virus Tegument Protein VP22 Contains an Internal VP16 Interaction Domain and a C-Terminal Domain That Are Both Required for VP22 Assembly into the Virus Particle

Wali Hafezi,† Emmanuelle Bernard, Rachelle Cook, and Gillian Elliott*

Marie Curie Research Institute, Oxted, Surrey, United Kingdom

Received 20 April 2005/Accepted 1 August 2005

Many steps along the herpesvirus assembly and maturation pathway remain unclear. In particular, the acquisition of the virus tegument is a poorly understood process, and the molecular interactions involved in tegument assembly have not yet been defined. Previously we have shown that the two major herpes simplex virus tegument proteins VP22 and VP16 are able to interact, although the relevance of this to virus assembly is not clear. Here we have constructed a number of recombinant viruses expressing N- and C-terminal truncations of VP22 and have used them to identify regions of the protein involved in its assembly into the virus structure. Analysis of the packaging of these VP22 variants into extracellular virions revealed that the C terminus of VP22 is absolutely required for this process, with removal of the C-terminal 89 residues abrogating its incorporation. However, while these 89 residues alone were sufficient for specific incorporation of small amounts of VP22 into the tegument, efficient packaging of VP22 to the levels of full-length protein required an additional 52 residues of the protein. Coimmunoprecipitation assays indicated that these 52 residues also contained the interaction domain for VP16. Furthermore, analysis of the subcellular localization of the mutant forms of VP22 revealed that only those truncations that were efficiently assembled formed characteristic cytoplasmic trafficking complexes, suggesting that these complexes may represent the cellular location for VP22 assembly into the virus. Taken together, these results suggest that there are two determinants involved in the packaging of VP22—a C-terminal domain and an internal VP16 interaction domain, both of which are required for the efficient recruitment of VP22 to sites of virus assembly.

Herpesviruses are large, enveloped viruses that contain a central DNA-containing capsid surrounded by a compartment known as the tegument (6). While herpesvirus maturation has been the subject of various studies in recent years, there are still many aspects of the virus assembly pathway that remain to be elucidated. It is well established that the capsid assembles in the nucleus of the cell, where it packages the DNA genome (32, 33), and that the assembling virus acquires its envelope from cytoplasmic membranes, most likely the trans-Golgi network or endosomal membranes (2, 20). However, the cellular site(s) of tegument acquisition is still to be established and there is now increasing evidence to suggest that subsets of tegument proteins may be added as assembly progresses along the maturation pathway (26). Hence, the tegument is more likely to be an organized structure than the amorphous layer it has so often been termed.

The herpes simplex virus (HSV) tegument is composed of a number of major and minor components, several of which, such as VP16, VP1/2, and UL37, have been shown to be essential to the virus (8, 9, 35). Other tegument proteins, such as VP13/14 and UL13, are nonessential to the process of virus replication in culture (5, 37), a feature that may be due in part to either functional redundancy among tegument proteins or cell type-specific requirements. Previous studies on the assembly of the major tegument protein VP22 have shown that overexpression of this protein in infected cells leads to an increase in its incorporation into the virus particle (24). This result may imply that the intracellular concentration of a particular tegument protein is the determining factor in its efficiency of packaging. However, tegument proteins may also contain specific packaging signals for assembly into the tegument, which could be involved in targeting these proteins to the correct subcellular sites for assembly and/or protein-protein interactions with other virus components. For example, a number of interactions have been demonstrated between tegument proteins VP16 and VP22 (12) and VP16 and vhs (34), suggesting that assembly of certain proteins may be controlled in part by their interactions with other components of the tegument. In addition, some tegument proteins have been shown to interact with the cytoplasmic tails of several glycoproteins, which may indicate a role for the envelope in recruiting the tegument (or vice versa) (18, 19).

The present study was concerned with the assembly mechanism of the major HSV type 1 (HSV-1) tegument protein VP22. We have previously shown that the fusion of green fluorescent protein (GFP) to VP22 in the context of virus infection has no effect on the replication properties of HSV-1 or the packaging of VP22 into the virion, and thus we have used live-cell fluorescence to investigate the subcellular localization of VP22 at different times in infection (15). Those studies have indicated that the localization patterns of VP22 in the infected cell are complex, consisting of diffuse cytoplasmic material early in infection, progressing to rapidly trafficking

* Corresponding author. Mailing address: Marie Curie Research Institute, The Chart, Oxted, Surrey RH8 OTL, United Kingdom. Phone: 44 1883 722306. Fax: 44 1883 714375. E-mail: g.elliott@mcri.ac.uk.

† Present address: Institute of Medical Microbiology and Interdisciplinary Center of Clinical Research (IZKF), University of Muenster, Muenster, Germany.

fluorescent complexes in the cytoplasm and intense fluorescence at the cell periphery at later times. In addition, we have shown that VP22 localizes to specific domains in the infected cell nucleus early in infection, where it is followed by the other tegument proteins VP13/14 and VP16 (21, 23). Although our results indicate that VP22 is predominantly cytoplasmic throughout infection, with small amounts present in the nucleus, contrasting results from other studies have suggested that the protein translocates to the nucleus in the middle of the replication cycle (30). Hence, VP22 subcellular localization is a complicated issue and it has not yet been possible to identify the cellular site(s) of VP22 incorporation into the assembling virions.

In a very recent study, we have demonstrated that HSV-1 lacking the VP22-encoding gene is defective for growth in epithelial cells but not Vero cells (11). Importantly, the absence of VP22 from the infected cell had no effect on the packaging of VP16 into the virus particle, suggesting that VP22 is not involved in VP16 recruitment. However, the Δ22 virus was unable to package the immediate-early protein ICP0 into its structure, and immunofluorescence studies indicated that ICP0 was incorrectly localized in the cytoplasm of cells infected with this virus (11). By contrast, in wild-type (WT)-infected cells ICP0 colocalized with the same trafficking complexes as VP22, providing us with the first real evidence that these complexes (or a subset of them) may be involved in virus assembly. In the present study, we have produced a panel of recombinant viruses encoding a number of N- and C-terminal truncations of VP22 fused to GFP and have used these viruses to analyze the requirement for specific regions of VP22 in its assembly into the virus particle. Our data provide a correlation between the abilities of VP22 to be efficiently packaged into the virion and to localize to cytoplasmic complexes. Furthermore, we show that VP16 interaction also correlates with assembly of VP22, suggesting that although VP22 is not involved in recruiting VP16, VP16 may play a role in recruiting VP22. Thus, by using VP22 as a marker for tegument assembly we have provided the first detailed description of the determinants required for the assembly of a major tegument protein into the HSV-1 virion.

MATERIALS AND METHODS

Cells, plasmids, and viruses. Vero and BHK cells were grown in Dulbecco's modified Eagle's medium supplemented with 10% newborn calf serum. Viruses were routinely grown in BHK cells or Vero cells and titrated on Vero cells. Extracellular virions were purified on Ficoll gradients from the infected cell medium of 5×10^8 BHK cells as described previously (15). Infectious virus DNA was also produced from extracellular virus as described previously (15).

The recombinant HSV-1 expressing GFP-tagged VP22 (166v) has been described previously (15). The VP22 deletion mutant (169v) that expresses GFP in place of VP22 has also been described recently (11). In the course of studying this virus, we isolated a mutant that expressed a nonfluorescing version of GFP, due to a single point mutation in the GFP open reading frame. This new virus, called 169vc, was utilized in the isolation of the recombinant viruses described below.

All other recombinant viruses used in this study were produced using plasmids based on the original plasmid pGE166 (15), which consists of GFP-VP22 in the flanking sequences of the *UL49* gene. Plasmid pGE193, expressing GFP fused to residues 1 to 212 of VP22, was constructed by inserting a stop codon at the NsiI site in pGE166. Plasmid pGE195, expressing GFP fused to residues 160 to 301 of VP22, was constructed by replacing the BsrGI-NsiI fragment of pGE166 with that from plasmid pGFP160-301 (25). The plasmid expressing GFP fused to residues 108 to 301 of VP22, pGE187, was constructed by digesting pGE166 with BspEI and religating the vector. To construct GFP fused to residues 1 to 165 of VP22 (pWH1), this region of the gene was amplified, a stop codon was incorporated, and the resulting product was used to replace the pPUM1/KpnI fragment of pGE166. pWH5 and pWH4 were constructing by replacing the AgeI-NsiI fragment of pGE166 with those from plasmids pGE192 and pGE191, respectively (25).

To obtain recombinant virus, the appropriate plasmid was cotransfected into Vero cells with infectious virus DNA from the VP22 deletion mutant, 169vc. Virus plaques were screened for GFP fluorescence using live-cell microscopy, and the resulting fluorescent viruses were plaque purified three times prior to production of master and working stocks.

Reagents and antibodies. Monoclonal antibodies to α-tubulin and HSV-1 major capsid protein VP5 were obtained from Sigma and Autogen Bioclear, respectively. Monoclonal and polyclonal anti-GFP antibodies were obtained from BD Biosciences Clontech. Anti-VP22 polyclonal antibody AGV031 was raised against glutathione *S*-transferase–VP22 expressed in *Escherichia coli* and has been shown previously to cross-react with only the N-terminal 60 residues of the protein. Anti-VP22 polyclonal antibody AGV600 was raised against His-tagged 257-301 of VP22 expressed in *E. coli* and thus is specific to the C terminus of the protein. Monoclonal anti-VP16 antibody (LP1) and monoclonal anti-gD antibody (LP14) were kindly provided by Helena Browne, Department of Pathology, Cambridge, United Kingdom. Polyclonal anti-VP13/14 antibody was kindly provided by David Meredith, University of Leeds.

One-step growth curves. Vero cells grown in a six-well plate (10^6 per well) were infected at a multiplicity of 10 in 1 ml medium per well. After 1 h (taken as 1 h postinfection), the inoculum was removed, the cells washed with phosphate-buffered saline (PBS), and 2 ml fresh medium added to each well. At a range of times after infection, one well of infected cells was harvested for total virus yield. Each virus sample was then titrated on Vero cells. All plaque assays were carried out in Dulbecco's modified Eagle's medium supplemented with 2% newborn calf serum and 1% human serum (Harlan Sera-Lab).

Sodium dodecyl sulfate (SDS)-polyacrylamide gel electrophoresis (PAGE) and Western blotting. Protein samples were analyzed on 10% polyacrylamide gels and electrophoresed in SDS-Tris-glycine buffer. Following electrophoresis, gels were either stained with Coomassie blue or transferred to nitrocellulose for analysis by Western blotting. Western blot assays were developed using enhanced chemiluminescence (Pierce).

Virion stripping experiments. Equivalent amounts of virions were pelleted at $2{,}300 \times g$ for 5 min at 4°C and resuspended in 50 μl of 10 mM Tris-HCl (pH 7.5)–1 mM EDTA–100 mM NaCl–1% NP-40. The virions were then incubated for 15 min at room temperature and pelleted again to separate the envelope fraction in the supernatant and the capsid-teguments in the pellet.

Immunoprecipitation assays. Vero cells grown in 6-cm dishes were infected with the relevant viruses at a multiplicity of 10. After 16 h, the cells were washed twice with PBS, solubilized in 1 ml RIPA buffer (50 mM Tris, pH 7.5, 150 mM NaCl, 0.1% SDS, 1% Na deoxycholate, 1% NP-40), and incubated on ice for 30 min. The cells were then centrifuged at $15{,}800 \times g$ for 30 min at 4°C and the supernatant collected. Half of each supernatant was made up to 1 ml with RIPA buffer and precleared on 40 μl protein A-Sepharose beads (50% slurry). Polyclonal anti-GFP antibody was added to the cleared lysates at a 1:200 dilution, and the mixture was incubated overnight at 4°C with rotation. A further 40 μl of protein A-Sepharose beads was added, the mixture was incubated for 4 h at 4°C with rotation, and the resulting protein A-antibody complexes were washed five times with wash buffer (50 mM Tris, pH 7.5, 150 mM NaCl, 0.1% NP-40). The immunoprecipitated proteins were then analyzed by Western blotting.

Live-cell fluorescence studies. Vero cells for fluorescence studies were grown in two-well Lab-Tek coverslip chambers (Quadrachem Laboratories). Infections of all GFP-tagged viruses were carried out at a multiplicity of 10, and images were subsequently acquired at various times using a Zeiss LSM400 confocal microscope. Resulting images were processed using Adobe Photoshop software.

Immunofluorescence. Vero cell grown on 16-mm coverslips were infected with the GFP-VP22-expressing virus (166v) at a multiplicity of 10 and fixed 8 h later with 4% paraformaldehyde. The cells were permeabilized by incubation for 15 min in PBS containing 0.5% Triton X-100, followed by washing with PBS. The cells were then blocked for 20 min in PBS containing 10% calf serum and incubated in the same solution containing VP16 monoclonal antibody LP1 at a dilution of 1 in 400 for a further 30 min. After extensive washing in PBS, the Texas Red-conjugated goat anti-mouse secondary antibody was added and the mixture was incubated for a further 20 min. After extensive washing with PBS, the coverslips were mounted in Vectashield (Vector Laboratories) and examined using a Zeiss LSM410 confocal microscope.

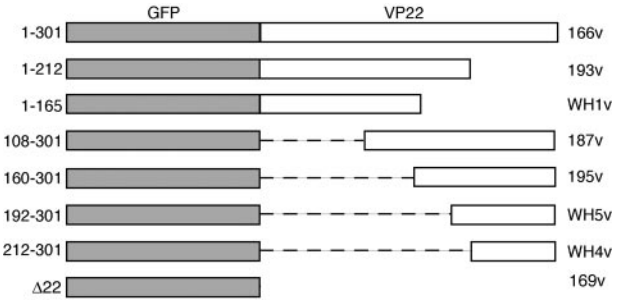

FIG. 1. Construction of viruses expressing GFP-tagged truncation mutant forms of VP22. The genes encoding the delineated fusion proteins were inserted into the flanking sequences of the VP22-encoding gene (*UL49*) and cotransfected into Vero cells with infectious DNA from the HSV-1 ΔVP22 virus expressing a nonfluorescing version of GFP (169vc). The resulting plaques were screened for GFP fluorescence and plaque purified three times prior to further analysis. Residues of VP22 encoded in the fusion proteins are indicated on the left. Virus names are shown on the right.

RESULTS

Construction of recombinant HSV-1 expressing truncation mutant forms of VP22 tagged with GFP. To construct recombinant viruses expressing a range of VP22 truncation mutant proteins, we transferred a number of GFP-tagged, truncated VP22 molecules from expression vectors used previously for transient-expression studies (25) into a plasmid containing the HSV-1 *UL49* gene flanking sequences (15). Each of these plasmids (Fig. 1) was cotransfected into Vero cells with infectious DNA from the HSV-1 VP22 deletion mutant (Δ22). Plaques were isolated and purified three times before the resulting viruses were grown and characterized by PCR analysis and sequencing of the mutated region of the genome. This resulted in a panel of viruses expressing N- and C-terminal truncations of VP22 that could be analyzed next to the virus expressing GFP-tagged full-length VP22 (166v) in the following series of experiments.

To assess the levels of VP22 expression from these viruses, monolayers of Vero cells were infected at a multiplicity of 10 with each virus and harvested 14 h after infection. Equal samples of each (as judged by the antitubulin loading control in Fig. 2A) were then analyzed by Western blotting with a number of antibodies specific for the GFP-VP22 proteins. Blotting with an anti-GFP antibody detected the VP22 variants from all the viruses (Fig. 2A, GFP) and showed that, with the exception of the virus expressing 1-212 of VP22, all the VP22 variants were expressed at approximately similar levels. In addition, a blot for major capsid protein VP5 indicated that this viral protein was expressed at equivalent levels in all the infections (Fig. 2A, VP5). We then confirmed the VP22 contents of the GFP fusion proteins using antibodies specific for both the N terminus and C terminus of VP22. As can be seen, the N-terminal antibody detected only the 1-212 and 1-165 variants (Fig. 2A, VP22 N-term) while the C-terminal antibody detected all the other VP22 variants (Fig. 2A, VP22 C-term). These blots also confirmed that, for an unknown reason, the 1-212 truncation of VP22 was expressed relatively poorly compared to the others, a result that is comparable to that obtained by others previously (29). Nonetheless, this variant of VP22 was easily detectable on slightly longer exposures of these Western blots.

To assess the replication efficiency of each of these viruses, one-step growth curves were determined with Vero cells. As we have previously shown that HSV-1 expressing GFP-VP22 in place of VP22 replicates as efficiently as the WT virus (15), we used this virus (166v) as our reference virus in this experiment. The replication rate for the Δ22 virus in Vero cells was shown to be similar to virus expressing full-length VP22 (Fig. 2B), a result that confirms our recent observation (11). Likewise, the replication rates for most of the other viruses expressing VP22 truncations were similar to virus expressing full-length VP22 (Fig. 2B). However, the viruses expressing residues 1 to 165 of VP22 (residues 1-165) or residues 192 to 301 of VP22 (residues 192-301) exhibited somewhat reduced replication efficiencies, resulting in an up to 10-fold reduction in virus yield (Fig. 2B). While the explanation for the growth defects exhibited by these two viruses is not clear, the fact that there is no defect in a VP22 knockout virus makes it likely that these variants of VP22 exert a dominant negative activity on virus replication. Nonetheless, all the viruses were shown to replicate to sufficient levels to enable purification of extracellular virus and analysis of virion protein content, as described below.

The N terminus of VP22 is dispensable for assembly into virions. We next addressed the question of which regions of VP22 are involved in packaging into the virus particle using our range of VP22 truncation mutant proteins. Our previous studies have indicated that full-length VP22 protein tagged with GFP is assembled into the tegument as efficiently as untagged VP22 (15), and therefore we postulated that our GFP-tagged VP22 variants would behave in a manner specific to the VP22 sequences present in these variants. To determine the requirement for the N-terminal region of VP22 in assembly of the protein into the virion, we first purified extracellular virions from the viruses expressing full-length GFP-tagged VP22 and the truncation mutant forms expressing 108-301 and 160-301 of VP22. Equal amounts of virions were analyzed by SDS-PAGE, and the gel was subsequently stained with Coomassie blue. Novel protein bands were clearly visible in the protein profiles of the mutant viruses at the approximately correct sizes of 48 and 42 kDa, respectively, and in amounts apparently similar to that present in virions containing full-length VP22 tagged with GFP (Fig. 3A, asterisks). To confirm that these proteins were the GFP-tagged, truncated VP22 molecules, we carried out Western blotting with an anti-VP22 antibody specific for the C terminus of VP22. These new components of the virions cross-reacted with the VP22 antibody, confirming their identity (Fig. 3B). Furthermore, the anti-VP16 blot indicated that the virions were equally loaded, and therefore these VP22 truncations were clearly assembled with an efficiency equal to that of full-length VP22 (Fig. 3B). Thus, we conclude that the N-terminal 160 residues of the VP22 molecule are entirely dispensable for its assembly into the virus.

The C terminus of VP22 is required for assembly into virions. We next examined the VP22 contents of virions produced by the two viruses expressing the C-terminal truncations of VP22, consisting of residues 1-212 and 1-165. The virion profiles from these viruses indicate that, unlike the full-length GFP-VP22 fusion that is easily detectable in the stained gel (asterisks in Fig. 4A and B), there are no protein bands ap-

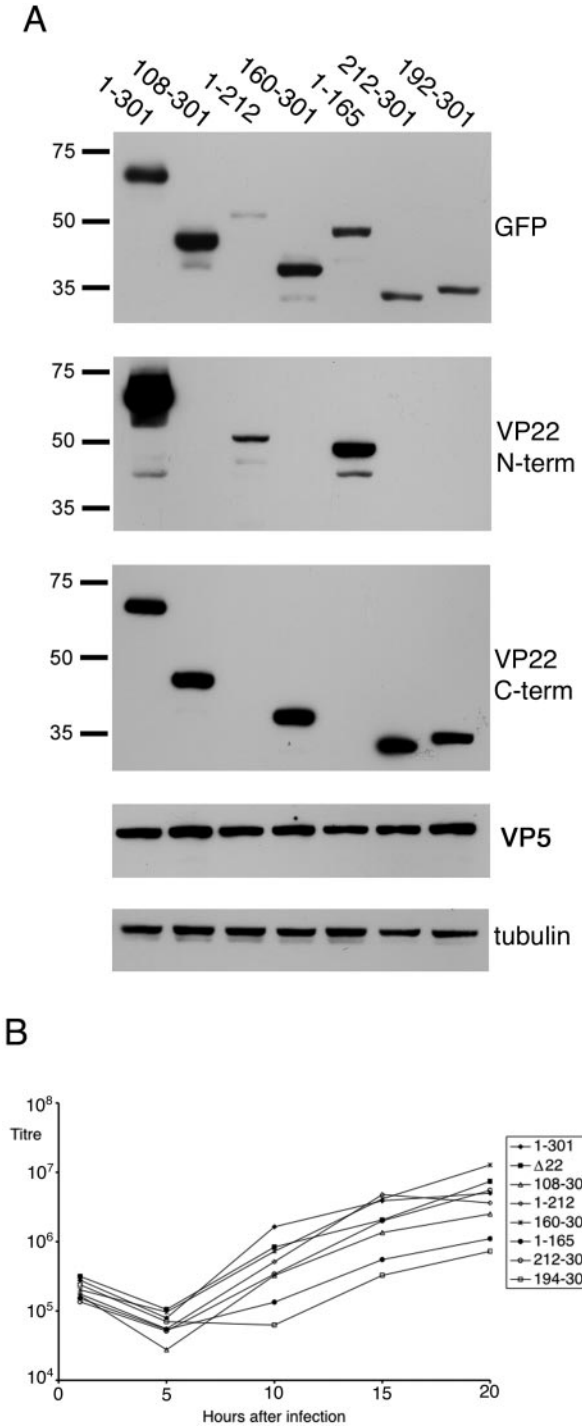

FIG. 2. Replication of viruses expressing truncation mutant forms of VP22. (A) Vero cells were infected with viruses expressing GFP-tagged truncation mutant forms of VP22 at a multiplicity of 10. Sixteen hours later, total cell extracts were analyzed by SDS-PAGE, followed by Western blotting with monoclonal anti-GFP antibody, polyclonal anti-VP22 antibodies specific for the N terminus or C terminus of the protein, and monoclonal anti-VP5 and -α-tubulin antibodies. The values on the left are molecular sizes in kilodaltons. (B) One-step growth curves of viruses expressing full-length VP22 or the truncation mutant forms of VP22 were determined by infecting monolayers of Vero cells with the viruses at a multiplicity of 10. At various times after infection, total virus was harvested by combining the cells and medium and titrated on Vero cells. The growth of the Δ22 virus was also analyzed in the same experiment.

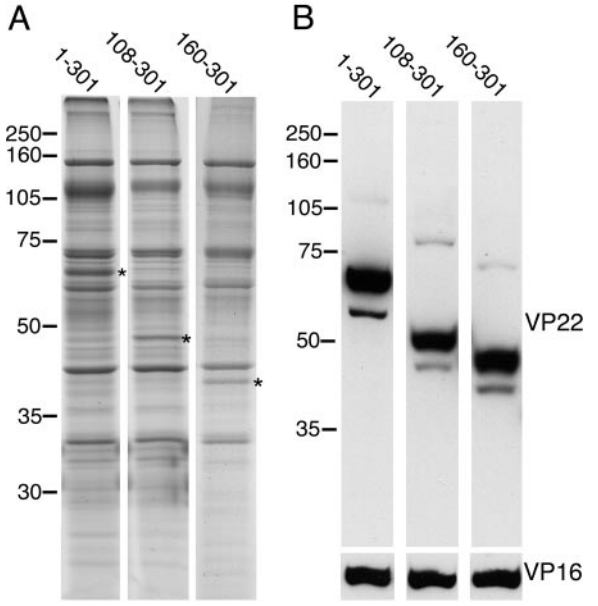

FIG. 3. The N terminus of VP22 is dispensable for assembly into the virion. Extracellular virions were prepared from cells infected with HSV-1 expressing GFP-tagged VP22 consisting of the full-length protein (residues 1-301), residues 108-301, or residues 160-301. Equivalent numbers of virions were analyzed by SDS-PAGE, followed by (A) Coomassie blue staining or (B) Western blotting with anti-VP22 or anti-VP16 antibodies. Asterisks denote the VP22-specific bands present in the virion profiles. The values on the left of each panel are molecular sizes in kilodaltons.

parent in the other two virion preparations of the sizes expected (50 and 44 kDa, respectively) for the two truncations. To determine if these molecules were packaged at levels not obvious above the background protein concentration in the stained gel, we next carried out a Western blot assay of the virions with an antibody specific for the N terminus of VP22 (Fig. 4C). While blotting with an antibody specific for tegument protein VP16 indicated that the virions were equally loaded on the gel, the anti-VP22 blot showed that there was no detectable amount of VP22 incorporated into the virions prepared from either of the mutant viruses (Fig. 4C). Although we have shown above that the 1-212 variant is expressed in infected cells at lower levels than full-length VP22, overexposure of the virion Western blot showed no evidence of this protein in the virion preparation, confirming that residues 1-212 of VP22 were not packaged into the virus. Thus, the C-terminal 89 residues of VP22 seem to be required for assembly of this protein into the virus particle.

Optimal packaging of VP22 requires the C-terminal 140 residues. To determine if the C-terminal 89 residues of VP22 are necessary and sufficient for packaging into the virion, we next analyzed virus that expressed only residues 212-301 of the C terminus. Once again, extracellular virions were analyzed by SDS-PAGE alongside virions containing full-length VP22, followed by either Coomassie blue staining or Western blotting of the protein gels. In this case, the Coomassie-stained gel showed that this virus did not package detectable amounts of VP22 into its virions (Fig. 5A, 212-301). However, Western blotting of the virions demonstrated that although the levels of

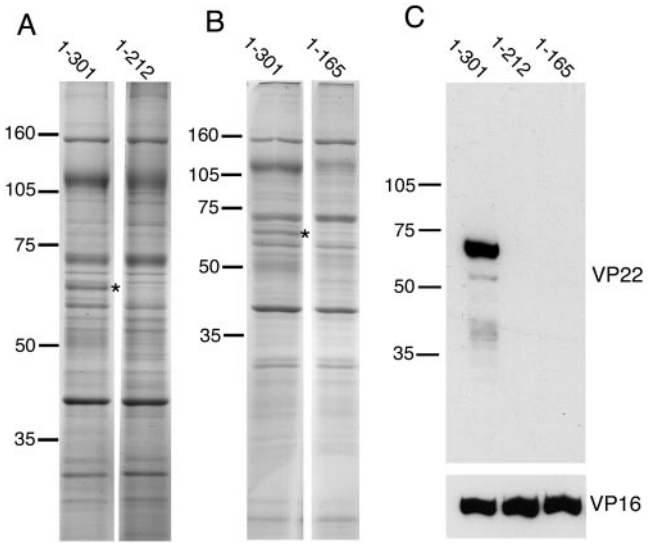

FIG. 4. The C terminus of VP22 is essential for assembly into the virion. Extracellular virions were prepared from cells infected with HSV-1 expressing GFP-tagged VP22 consisting of the full-length protein (residues 1-301), residues 1-212, or residues 1-165. Equivalent numbers of virions were analyzed by SDS-PAGE, followed by (A and B) Coomassie blue staining or (C) Western blotting with anti-VP22 or anti-VP16 antibodies. Asterisks denote the full-length GFP-VP22 band present in the virion profile. The values on the left of each panel are molecular sizes in kilodaltons.

VP22 were greatly reduced in these virus particles, the levels were detectable with the anti-VP22 antibody when the blot was slightly overexposed (Fig. 5B). Taken together with our previous finding that the C-terminal 140 residues of VP22 are packaged as efficiently as full-length VP22 (160-301 in Fig. 3), these results seem to indicate that the region between residues 160 and 212 is essential for efficient packaging of VP22 into the virus particle. To determine if we could refine this region further, we next investigated the packaging levels of an intermediate truncation, encoding residues 192-301. As for the 212-301 variant, the Coomassie-stained virions of the 192-301 variant did not show any evidence of a packaged VP22 molecule (Fig. 5A, 192-301). In addition, the Western blot showed reduced but detectable levels of this protein in the virion preparation (Fig. 5C), similar to the levels seen for the 212-301 variant.

These results show that the C-terminal 89-residue region of VP22 has the ability to be packaged into the virus, albeit at much lower levels than the full-length protein. To ensure that this C-terminal peptide was specifically assembled into the tegument, we used detergent treatment to fractionate extracellular virions from virus expressing full-length VP22, the C-terminal 89 residues of VP22, or the C-terminal 109 residues of VP22 into envelope and tegument-capsid fractions. Western blot assays were then carried out on these fractions and reacted with antibodies specific for the envelope protein gD and the tegument protein VP13/14. The blots with the gD and VP13/14 antibodies demonstrated that in all cases, the fractionation had successfully produced an envelope fraction containing gD and a tegument-capsid fraction containing VP13/14 (Fig. 5D). Furthermore, blotting for GFP showed that, as expected, the full-length GFP-VP22 fusion protein fractionated in the tegument-capsid fraction of the virions (Fig. 5D, 1-301). GFP blotting of the virions containing the C-terminal regions of VP22 also showed that this region of VP22 was packaged into the tegument of the virus, confirming that GFP fused to the C terminus of VP22 contained enough information for assembly into the tegument (Fig. 5D, 192-301 and 212-301).

To ensure that GFP alone was not capable of being packaged into the tegument, we carried out the same analysis on virions purified from our Δ22 virus that expresses GFP in place of VP22. In this case we found, somewhat surprisingly, that GFP was present in the Δ22 virion preparation (Fig. 5D, Δ22, lane T). However, while GFP fused to the C terminus of VP22 was specifically assembled into the tegument of the virion (Fig. 5D, 212-301), all unfused GFP associated with the Δ22 virions was readily released in the envelope fraction (Fig. 5D, Δ22). To investigate this further, Δ22 and GFP-VP22-containing virions were fractionated on a Ficoll gradient and 10 individual fractions collected across each gradient. Each fraction was then titrated to determine the presence of infectious virus across the gradient and assessed by Western blotting for the presence of capsids (VP5 blot) and GFP to correlate protein content with infectivity. These results revealed that in a Ficoll gradient used to prepare GFP-VP22-containing virions, the level of GFP in the fractions correlated directly with the presence of capsids and infectivity in the gradient, and hence the GFP-VP22 copurified with GFP-VP22 virions (Fig. 5E, GFP-VP22). By contrast, GFP levels were consistently high in all fractions of a Ficoll gradient used in the preparation of the Δ22 virions and did not correlate with either the capsid content or the relative infectivity across the gradient (Fig. 5E, Δ22). Thus, we believe the presence of GFP in the Δ22 virion preparation is purely a reflection of the well-established soluble nature of this protein in the cell, which probably results in the protein being released at high levels into the medium of infected cells once they have been lysed.

In summary, we interpret these results to mean that there are two regions of VP22 involved in its packaging into the virus—residues 212-301 can be assembled into the tegument in small amounts, while residues 160-192 are required to enhance this level of assembly to that observed for the full-length protein. Although we cannot rule out the possibility that residues 212-301 are packaged into the virion in an undirected random manner, we believe the specific incorporation of this region into the tegument indicates that a specific interaction is involved in its assembly.

Interaction of truncation mutant forms of VP22 with VP16. We have previously shown that VP22 can interact with a second major tegument protein, VP16 (12), but that the absence of VP22 from the virus has no effect on the packaging of VP16 into the virion (11). To investigate a potential role for VP16 in the assembly of VP22, we first determined the localization of VP16 in relation to GFP-VP22 in the infected cell. Vero cells were infected at a multiplicity of 10 with HSV-1 expressing full-length VP22 fused to GFP and fixed 8 h after infection, and an immunofluorescence assay was carried out for VP16. While there was a much higher level of VP16 in the nucleus of the infected cell compared to GFP-VP22, the cytoplasmic localizations of the two tegument proteins were very similar (Fig. 6A, compare GFP-VP22 with VP16). Overlaying the images

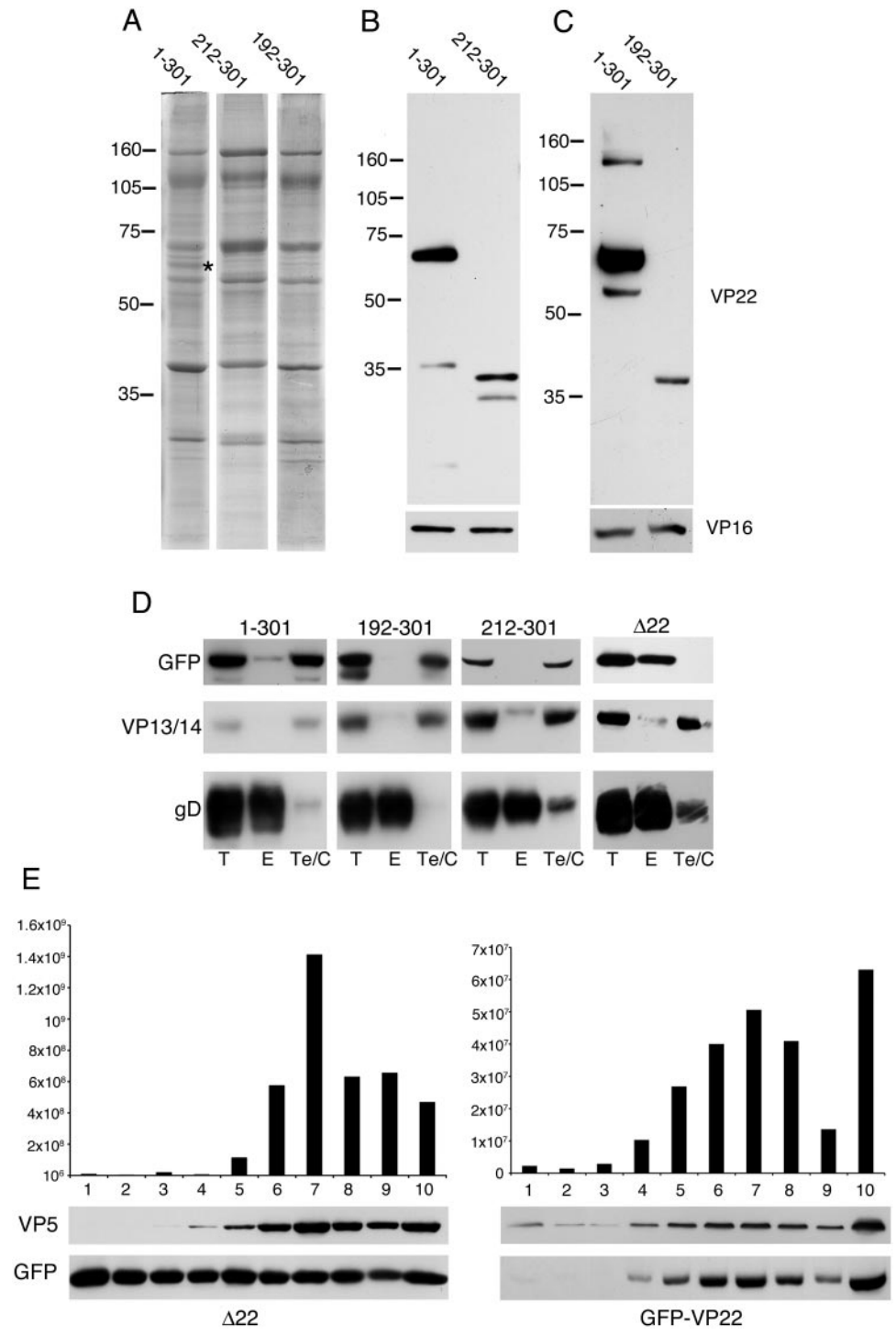

FIG. 5. Assembly properties of the extreme C terminus of VP22. Extracellular virions were prepared from cells infected with HSV-1 expressing GFP-tagged VP22 consisting of the full-length protein (residues 1-301), residues 212-301, or residues 192-301. Equivalent numbers of virions were analyzed by SDS-PAGE, followed by (A) Coomassie blue staining or (B and C) Western blotting with anti-VP22 or anti-VP16 antibodies. The asterisk denotes the full-length GFP-VP22 band present in the virion profile. (D) Extracellular virions from HSV-1 expressing GFP fused to residues 1-301, 192-301, or 212-301 of VP22 or expressing GFP in place of VP22 (Δ22) were subjected to fractionation into envelope and tegument-capsid fractions by detergent treatment of intact virus particles. Following separation of detergent-soluble (envelope) and detergent-insoluble (tegument-capsid) fractions, the samples were analyzed by SDS-PAGE, followed by Western blotting with antibodies specific for envelope (anti-gD), tegument (anti-VP13/14), and GFP. T, total; E, envelope fraction; Te/C, tegument-capsid fraction. (E) Extracellular virions from BHK21 cells infected with either the Δ22 virus or the GFP-VP22-expressing virus were fractionated on a 5 to 15% Ficoll gradient. Ten fractions across the entire gradient were collected and analyzed by titration on Vero cells or by Western blotting using antibodies for GFP and VP5. Fraction 1 represents the top of the gradient, fraction 10 the bottom. The values on the left of panels A, B, and C are molecular sizes in kilodaltons.

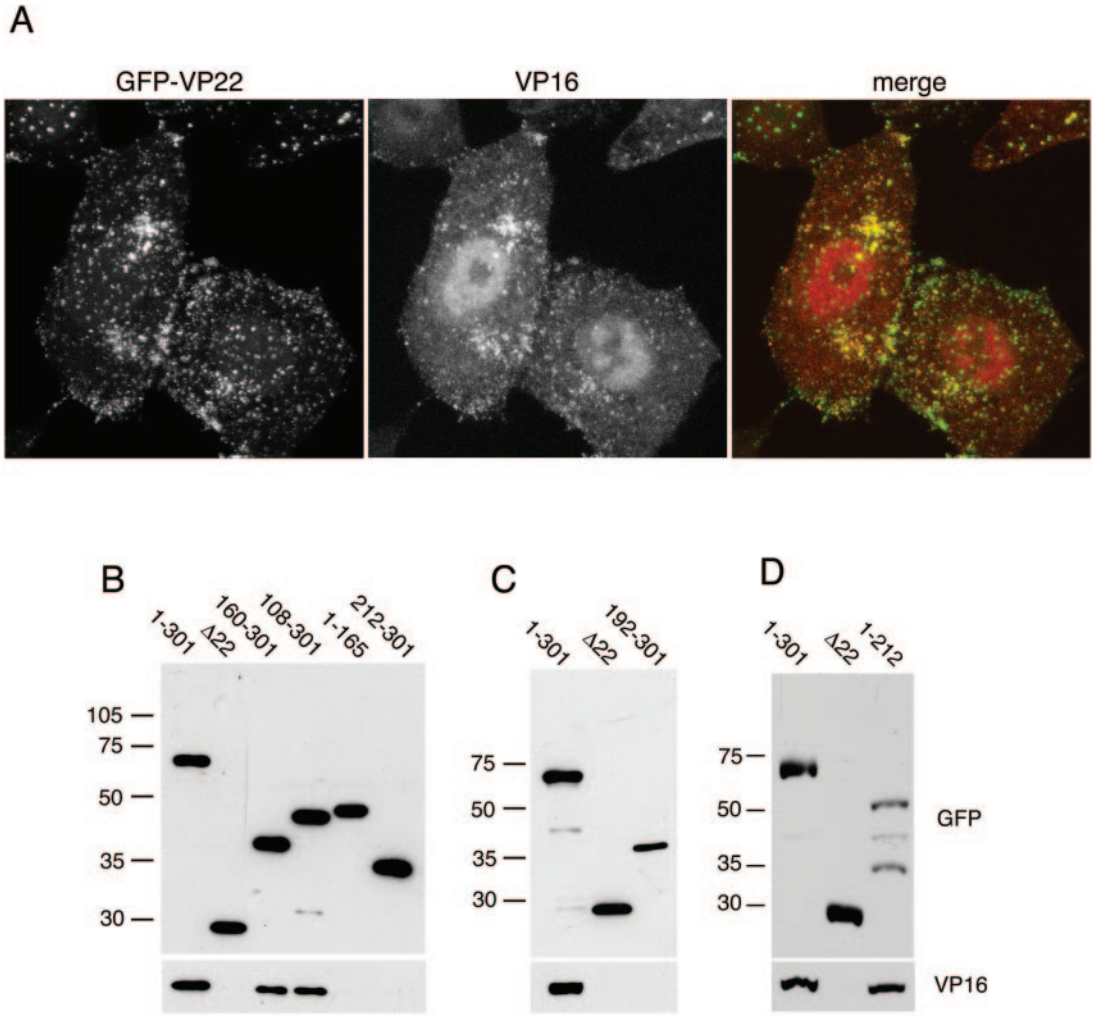

FIG. 6. Correlation between VP16 interaction and assembly of VP22 into the virion. (A) VP16 colocalizes with GFP-VP22 in infected cells. Vero cells infected with 166v at a multiplicity of 10 were fixed 8 h after infection and processed for immunofluorescence with anti-VP16 monoclonal antibody LP1. (B, C, and D) Vero cells infected with viruses expressing the indicated GFP-VP22 fusion proteins were solubilized with RIPA buffer and immunoprecipitated with a polyclonal anti-GFP antibody. The resulting immunocomplexes were analyzed by SDS-PAGE and Western blotting with a monoclonal anti-GFP antibody to detect precipitated GFP fusion proteins and a monoclonal anti-VP16 antibody to detect coimmunoprecipitated VP16. Δ22 denotes HSV-1 that expresses GFP in place of the entire VP22-encoding gene. Because of its poor expression level, the 1-212 variant of VP22 was immunoprecipitated from fivefold more cells. The values on the left of panels B, C, and D are molecular sizes in kilodaltons.

indicated that a large population of VP16 colocalized with the characteristic cytoplasmic complexes observed for GFP-VP22, suggesting that the two proteins were in the same complexes within the infected cell (Fig. 6A, merge).

We next wished to establish if there was a correlation between VP22 packaging and its ability to interact with VP16 by conducting coimmunoprecipitation assays on infected cell extracts. Vero cells infected with viruses expressing either full-length VP22 tagged with GFP (1-301), the truncation mutant forms of VP22 tagged with GFP, or GFP in place of VP22 (Δ22) were harvested 16 h after infection and total cell extracts prepared in RIPA buffer. All GFP-containing proteins were then immunoprecipitated with a polyclonal anti-GFP antibody and analyzed by Western blotting with both a monoclonal anti-GFP antibody to determine the efficiency of immunoprecipitation and a monoclonal anti-VP16 antibody to determine the level of VP16 interacting with each mutant form of VP22. All the mutants of GFP-VP22 were present in each extract at equivalent levels (data not shown) and were precipitated by the GFP antibody (Fig. 6B, C, and D, GFP). VP16 was also present in all the infected cell extracts at similar levels (data not shown) and was coimmunoprecipitated efficiently with full-length VP22 (Fig. 6B, C, and D, 1-301). By contrast, precipitation of GFP alone from the Δ22 virus-infected cells did not coprecipitate VP16, confirming that the result obtained with full-length VP22 was due to a specific interaction with VP16 (Fig. 6B, C, and D, Δ22). Interestingly, VP16 was efficiently coprecipitated from cells infected with the viruses expressing the N-terminal truncations 108-301 and 160-301 (Fig. 6B). However, VP16 was not precipitated from extracts of cells infected with the two viruses that express the C-terminal regions of VP22, 212-301 (Fig. 6B) and 192-301 (Fig. 6C), suggesting that the region between residues 160 and 192 is required for interaction with VP16. Furthermore, while VP16

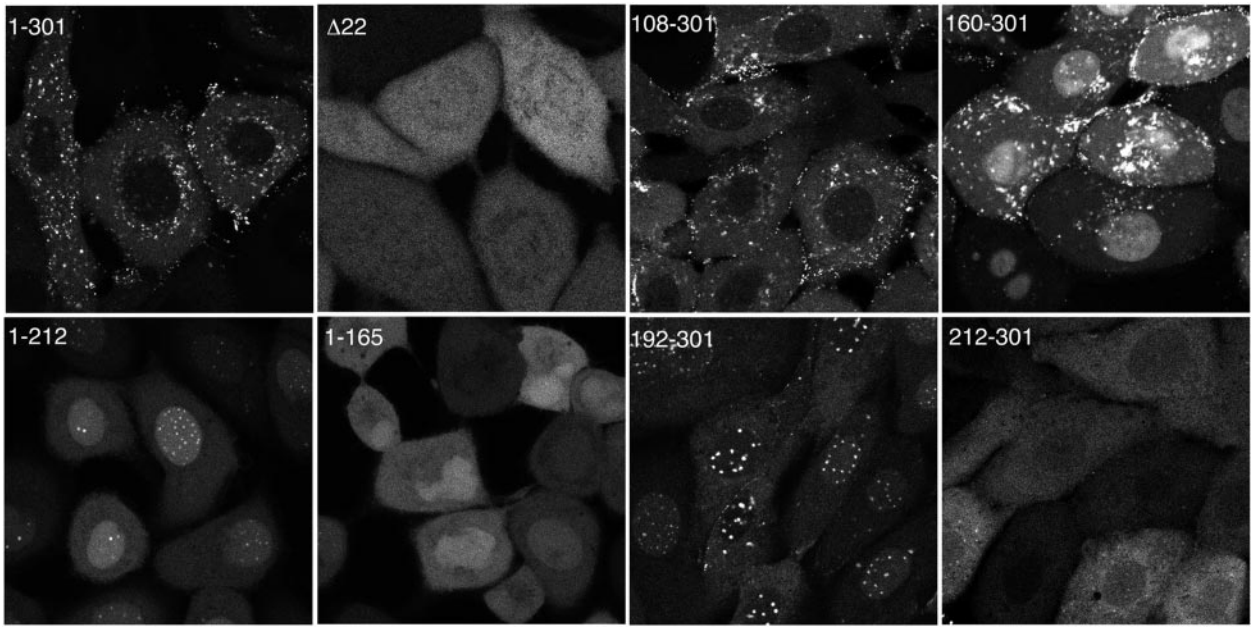

FIG. 7. Assembly into the virion correlates with localization to cytoplasmic complexes. Confluent Vero cells grown in coverslip chambers were infected with each of the indicated viruses at a multiplicity of 10. Around 8 to 10 h after infection, representative images of the GFP fluorescence present in each monolayer of live infected cells were acquired using a Zeiss LSM-410 confocal microscope. Δ22 denotes HSV-1 that expresses GFP in place of the VP22-encoding gene (*UL49*). The image for 1-212 was acquired using threefold higher laser power.

coprecipitated efficiently with 1-212 of VP22 (Fig. 6D) we could not detect any VP16 present in the complexes precipitated from cells infected with virus expressing 1-165 of VP22 (Fig. 6B). Hence, taken together these results imply that the VP16 interaction domain of VP22 is contained in the internal region between residues 160 and 212. In addition, while the two truncations of VP22 that are packaged in the structure of the virus to WT levels were able to interact with VP16 (108-301 and 160-301), one variant (1-212) interacted efficiently with VP16 but was not packaged, implying that VP16 interaction may be necessary but not sufficient for incorporation of VP22 into the virion.

Localization of truncation mutant forms of VP22 in virus-infected cells. The requirement for a specific region of VP22 for assembly into the virus may reflect any of a number of aspects of VP22 biology, including the need for specific subcellular targeting of the protein during the virus assembly process. As we have described previously, the localization of full-length GFP-22 in live infected cells is complex, with it localizing to a number of characteristic subcellular sites including trafficking complexes in the cytoplasm and specific punctate sites in the nucleus (15, 21). It has not been possible to distinguish which of these sites is the location of VP22 assembly into the virus. In an attempt to correlate subcellular localization with packaging into the virus, we next investigated the cellular localization patterns of the various truncation mutant forms of VP22 in live, virus-infected cells. When we examined the localization of the two N-terminal truncations, we noted that the mutant form of VP22 expressing residues 108-301 had an appearance similar to that of full-length VP22, with both proteins being concentrated mainly in the cytoplasm of the cell (Fig. 7, compare 1-301 and 108-301). In addition, both the full-length protein and the 108-301 mutant form localized to punctate nuclear domains in small amounts (Fig. 8, compare 1-301 and 108-301). It is noteworthy that this truncation mutant form is small enough to passively diffuse through the nuclear pore complex into the nucleus (48 kDa) but, like full-length GFP-VP22, is in fact predominantly cytoplasmic, confirming our previous findings on the relative targeting of VP22 to the cytoplasm or nucleus (25). By contrast, the mutant form of VP22 expressing residues 160-301 was clearly present at much higher levels in the nucleus of the cell, where it localized to the nucleoplasm, replication compartments, and punctate domains (Fig. 7 and 8, 160-301). However, there was also a high level of fluorescence in the cytoplasm of cells infected with this virus which was specifically localized in trafficking complexes similar to those observed in cells infected with virus expressing full-length and residues 108-301 of VP22 (Fig. 7, 160-301).

We next examined the localization patterns of the two C-terminal truncations that we have shown above are not assembled into the virus. Like the variant 160-301, both the C-terminal truncations of VP22 (residues 1-212 and residues 1-165) were concentrated in the nucleus of the cell. However, unlike 160-301, the two C-terminal truncations exhibited only a diffuse localization in the cytoplasm of the infected cell (Fig. 7, compare 1-212 and 1-165 with 1-301), suggesting that neither of them was capable of specific targeting to the characteristic cytoplasmic complexes observed above. Interestingly, while residues 1-212 localized to the characteristic punctate domains in the nucleus, residues 1-165 exhibited only diffuse nuclear fluorescence, suggesting an involvement of sequences between 165 and 212 in targeting to these nuclear domains (Fig. 8, compare 1-212 and 1-165). The requirement for nuclear do-

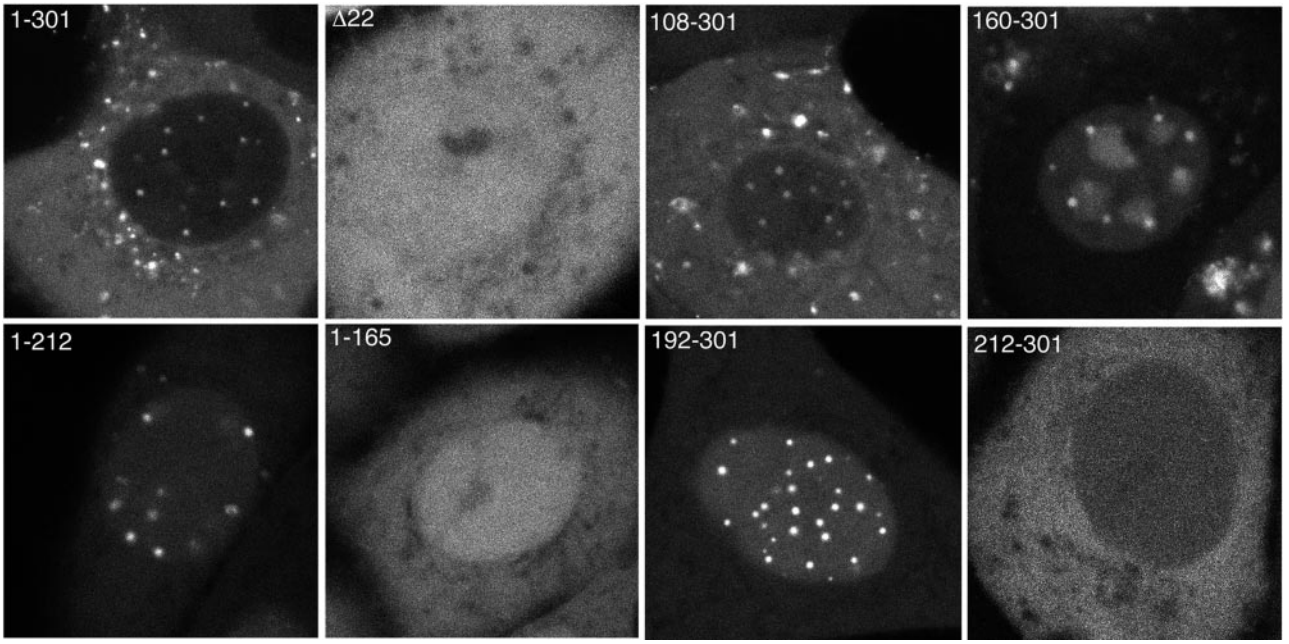

FIG. 8. Assembly into the virion does not correlate with localization to nuclear dots. Confluent Vero cells grown in coverslip chambers were infected with each of the indicated viruses at a multiplicity of 10. Around 8 to 10 h after infection, representative images of the GFP fluorescence present in the nuclei of live infected cells were acquired using a Zeiss LSM-410 confocal microscope. Δ22 denotes HSV-1 that expresses GFP in place of the VP22-encoding gene (*UL49*). The image for 1-212 was acquired using threefold higher laser power.

main targeting was refined even further by the results obtained with the last two VP22 variants, namely, residues 192-301 and 212-301. Live-cell imaging of Vero cells infected with these two viruses revealed that 192-301 localized very efficiently to nuclear domains, while 212-301 exhibited no such specific targeting in the nucleus (Fig. 7 and 8, compare 192-301 and 212-301). Furthermore, these proteins, which are only assembled into the virus at low levels, exhibited no specific targeting in the cytoplasm of the cell (Fig. 7, compare 192-301 and 212-301). In summary, the only variants of VP22 to be assembled efficiently into the virus were those that have the ability to interact with VP16 and localize to cytoplasmic complexes in the same manner as full-length VP22 (see Fig. 9A). Hence, we suggest that these sites represent the cellular location of VP22 incorporation into the virus particle and that VP16 may be involved in its recruitment.

DISCUSSION

The pathway of herpesvirus tegument assembly is poorly defined, and it is not clear in which compartment(s) of the cell the virus acquires its tegument proteins. In recent years, it has become obvious that many tegument proteins are likely to be multifunctional, with roles to play in early and late stages of virus replication. Hence, unlike the simple requirement for nuclear targeting by capsid proteins or membrane targeting by envelope proteins, the intracellular targeting of tegument proteins is complex and likely to be indicative of subcellular functional sites, as well as tegumentation sites. Indeed, the major tegument proteins VP16, VP22, and VP13/14 have all been shown to exist in both nuclear and cytoplasmic populations in the infected cell and furthermore in specific subpopulations within these compartments (10, 13, 15, 21, 23, 30). Because of the complex localization patterns of tegument proteins, it has not been possible to discern the subcellular population that represents assembling virus rather than protein trafficking through the cell for other purposes.

A number of approaches have been used previously to broadly address the mechanism and location of tegument protein incorporation into the assembling virus. These have included the biochemical fractionation of cellular compartments and membranes to measure the presence of tegument proteins and infectious virus, leading to the suggestion that mature virus assembles in the membranes of the trans-Golgi network or endosomal compartments (20). In addition, a number of elegant electron microscopy studies of pseudorabies viruses (PRVs) with their tegument proteins deleted have established a compelling model for the sequential addition of tegument proteins as the assembling virion is transported from the nuclear envelope to the cytoplasmic membranes involved in envelopment (16-18, 22). Interestingly, another recent study on PRV virions has demonstrated heterogeneity in the content of GFP-VP22 between individual particles (7). These authors have suggested that rather than being acquired by the assembling virion as individual molecules, GFP-VP22 may be recruited onto capsids in aggregates or patches.

Apart from one study on a large truncation mutant form of the UL41-encoded vhs protein that has identified a region within this protein required for its packaging (31), few studies have addressed the specific regions of individual tegument proteins required for their interaction with other virion proteins and assembly into the maturing virus. Here we provide the first detailed mutational analysis of a major HSV-1 tegument protein, the *UL49*-encoded VP22 protein, in the context

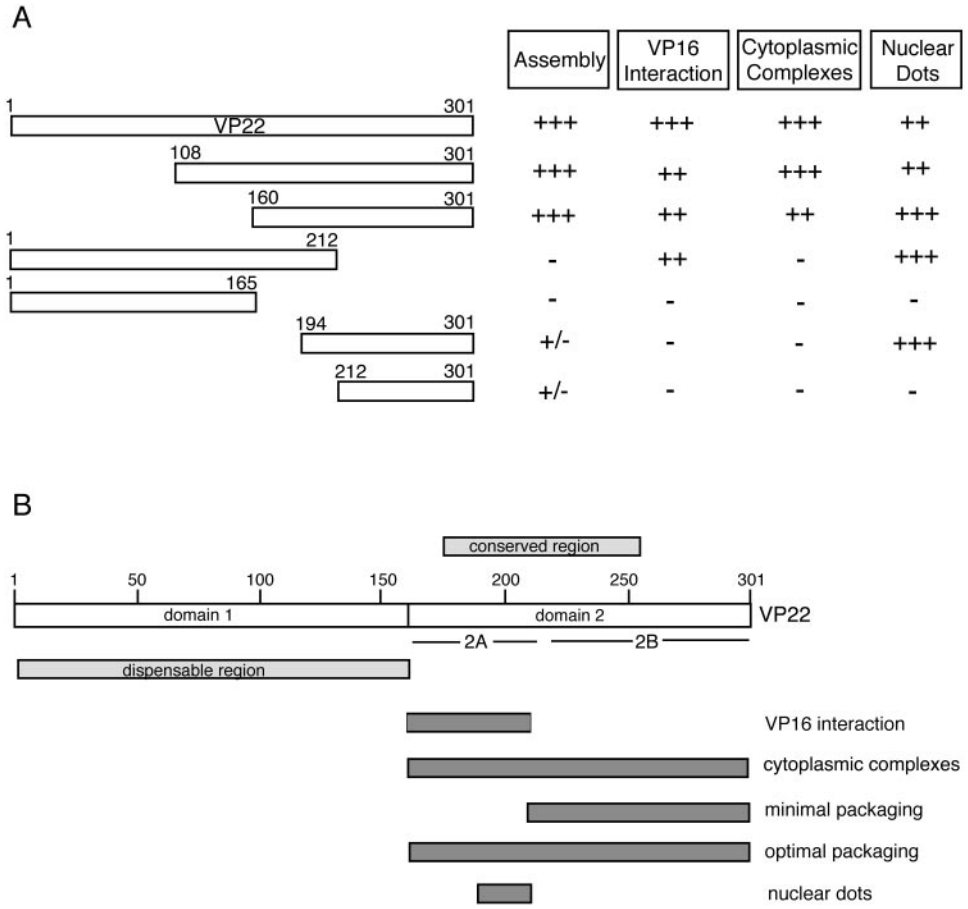

FIG. 9. Domains in VP22. (A) Summary of the behavior of the VP22 truncations used in this study. (B) Line drawing of VP22 indicating the regions of the protein involved in intracellular targeting, VP16 interaction, and packaging into the virus particle.

of virus infection. In this study, the genes encoding the truncation mutant forms of VP22 were all recombined into the virus genome in place of the parental gene at its natural locus. Furthermore, all the truncations were tagged with GFP so that the trafficking of the individual variants could be compared to that of GFP-tagged full-length VP22 (15). In this way, we have been able to correlate the ability of the VP22 variants to be assembled into the virus with their subcellular localization patterns (Fig. 9A). Our results indicate that only those variants that localized to specific cytoplasmic complexes were incorporated into the virus tegument at levels equivalent to the full-length protein, suggesting that assembly and cytoplasmic complex targeting are closely linked. Furthermore, our results suggest that VP22 must also be able to interact with VP16 to be targeted to these cytoplasmic complexes (Fig. 9A).

The results presented here complement a previous study we carried out on the same truncation mutant forms of VP22 expressed in transfected cells rather than during infection (25). This previous study demonstrated the complexity of VP22 subcellular localization expressed in isolation, and we identified a number of specific domains within the protein that seem to dictate its steady-state localization pattern. Our transfection studies indicated that the same region that we have shown here to be important for assembly, which incorporates the conserved core domain of the protein (Fig. 9B), was also involved in the activities of VP22 within transfected cells. In addition, the localization of the mutant forms of VP22, with respect to their relative cytoplasmic or nuclear compartmentalization, were the same in infected and transfected cells, suggesting that this is an intrinsic property of the protein. The assembly characteristics of the various VP22 truncations have enabled us to define regions within VP22 that are involved in its packaging into the tegument. While the N-terminal 160 residues (domain 1) are entirely dispensable for both incorporation into the virus and interaction with VP16, the C-terminal half of VP22 is required for assembly of VP22 to WT levels and interaction with VP16 (domain 2 and optimal packaging domain in Fig. 9B). Based on our coimmunoprecipitation studies of VP16 with VP22, we believe that domain 2 can be further divided into two subregions—domain 2A (residues 160-212) contains the VP16 binding region, while domain 2B, encompassing the C-terminal 89 residues, is not required for VP16 interaction but is absolutely essential for assembly of VP22 into the tegument. Both domains 2A and 2B are required for localization of VP22 to cytoplasmic trafficking complexes and efficient assembly into the tegument, but domain 2B alone is sufficient for packaging small amounts of VP22 specifically into the tegument. It should be noted that a previous study on a single truncation mutant form of VP22 lacking the C-terminal 89 residues (our domain 2B) has concluded, in contrast to our

results, that the N-terminal 212 residues of VP22 are packaged into virions (29). The reason for the discrepancy between the two studies is not clear, but the level of the truncated protein detected in the virions preparation in that study was so low that it may simply represent cellular contamination of the virions.

It is possible that the packaging of C-terminal residues 212-301) occurs by a random undirected mechanism. However, because of the apparent differential requirement for the two C-terminal regions of VP22, we would postulate that the targeting and assembly of VP22 require an interaction with at least two partners (viral and/or cellular) through the two domains in VP22. The first of these partners (interacting with domain 2A) is likely to be the major tegument protein VP16, as we have shown that VP22 and VP16 colocalize in the cytoplasm of the infected cell and coprecipitate from infected cell extracts. In addition, we have not yet found a mutant form of VP22 that is packaged to WT levels but does not interact with VP16. However, confirmation of the involvement of VP16 in VP22 assembly will require the exact determination of the VP16 binding site in VP22 (or vice versa), followed by the generation of a virus expressing VP22 specifically mutated in this region. The second partner of VP22 would interact with domain 2B, which is not required for or involved in the VP16 interaction. This interaction alone would be sufficient to bring small amounts of VP22 into the virus, potentially by a chance interaction between the C terminus of VP22 present in the cytosol and its partner. However, efficient assembly of VP22 would require the VP16 interaction in domain 2A in addition to the domain 2B interaction. Interestingly, the C terminus of the PRV homologue of VP22 has been shown to interact with the cytoplasmic tails of glycoproteins gE and gM (18), raising the possibility that a C-terminal partner of VP22 is an envelope protein. In support of this, it has recently been demonstrated that HSV-1 VP22 interacts with the cytoplasmic tail of glycoprotein gD (4), and our own recent studies on an HSV-1 knockout for VP22 have shown that the level of gD in the virion is reduced in the absence of VP22 (11).

While interactions between virus structural proteins are likely to be important for virus assembly, the targeting of VP22 to the correct cellular location for virus assembly may also involve an interaction with a cellular protein. We have previously shown that VP22 interacts with the cellular microtubule network when expressed in isolation (14, 25), and while the significance of such an interaction for virus replication is not clear, there is some evidence to suggest an involvement of microtubules in virus maturation, particularly in neurons (27, 28). In addition, transiently expressed VP22 has also been shown to associate with cellular membranes, and most probably the trans-Golgi network, a property that could also be important for assembly of this protein into the virus (1).

In the course of these studies, we have also assessed the ability of the truncation mutant forms of VP22 to localize to characteristic nuclear sites that we have previously identified as specific domains that lie adjacent to ND10 bodies (21). While the function of these nuclear sites is not yet clear, it has recently been reported that similar domains within the nucleus contain cellular chaperone proteins and components of the proteasomal machinery (3), and the authors of that report have suggested that such sites may facilitate protein quality control in the nucleus. The results presented here identify the 20 amino acids between residues 192 and 212 of VP22 as being critical for targeting of VP22 to these sites (Fig. 9B), and hence it seems that this protein might be specifically recruited to these domains. Furthermore, VP22 localizes to these sites even when it is present in the nucleus at very low levels (as in the case of 1-301 and 108-301 in Fig. 8), suggesting that concentration levels in the nucleus are not a factor in targeting to these domains.

In a very recent report, we have described the characterization of a recombinant HSV-1 that lacks the VP22-encoding gene (11). The major effects that we observed in this virus were an alteration in the localization and virion packaging of ICP0, suggesting that VP22 is involved in the subcellular targeting and incorporation of ICP0 into the virus particle. Hence, we are now beginning to build a detailed picture of the relative interactions involved in the assembly of the tegument, with VP16 involved in recruiting VP22, and VP22 subsequently involved in recruiting ICP0. Furthermore, we have shown that the localization of two tegument proteins (VP22 and ICP0) to the same trafficking complexes correlates with their assembly into the virion, strongly suggesting that these complexes represent a subcellular site of tegument protein assembly. We have also shown here that VP16 colocalizes in these complexes, and similar complexes were previously observed with a virus expressing the tegument protein UL46 fused to GFP (36). Given our current understanding of virus assembly, it is likely that these sites represent vesicles in the trans-Golgi network or endosomal compartments of the secretory pathway, but further studies must be carried out to confirm this. Nonetheless, using mutational analysis studies such as the ones described here we hope to reach a definition of where in the cell and through which protein-protein interactions at least one major tegument protein is packaged into the virion.

ACKNOWLEDGMENTS

We thank Helena Browne for anti-VP16 and anti-gD antibodies and David Meredith for anti-VP13/14 antibody.

W.H. was funded by Innovative Medizinische Forschung (HA620202) and Interdisciplinary Center of Clinical Research (Küh 3/064/04). E.B., R.C., and G.E. were funded by Marie Curie Cancer Care.

REFERENCES

1. **Brignati, M. J., J. S. Loomis, J. W. Wills, and R. J. Courtney.** 2003. Membrane association of VP22, a herpes simplex virus type 1 tegument protein. J. Virol. **77:**4888–4898.
2. **Brunetti, C. R., K. S. Dingwell, C. Wale, F. L. Graham, and D. C. Johnson.** 1998. Herpes simplex virus gD and virions accumulate in endosomes by mannose 6-phosphate-dependent and -independent mechanisms. J. Virol. **72:**3330–3339.
3. **Burch, A. D., and S. K. Weller.** 2004. Nuclear sequestration of cellular chaperone and proteasomal machinery during herpes simplex virus type 1 infection. J. Virol. **78:**7175–7185.
4. **Chi, J. H., C. A. Harley, A. Mukhopadhyay, and D. W. Wilson.** 2005. The cytoplasmic tail of herpes simplex virus envelope glycoprotein D binds to the tegument protein VP22 and to capsids. J. Gen. Virol. **86:**253–261.
5. **Coulter, L. J., H. W. Moss, J. Lang, and D. J. McGeoch.** 1993. A mutant of herpes simplex virus type 1 in which the UL13 protein kinase gene is disrupted. J Gen. Virol. **74**(Pt. 3)**:**387–395.
6. **Dargin, D.** 1986. The structure and assembly of herpes viruses, p. 359–437. *In* J. R. Harris and R. W. Horne (ed.), Electron microscopy of proteins, volume 5, virus structure, vol. 5. Academic Press, London, United Kingdom.
7. **del Rio, T., T. H. Ch'ng, E. A. Flood, S. P. Gross, and L. W. Enquist.** 2005. Heterogeneity of a fluorescent tegument component in single pseudorabies virus virions and enveloped axonal assemblies. J. Virol. **79:**3903–3919.
8. **Desai, P., G. L. Sexton, J. M. McCaffery, and S. Person.** 2001. A null mutation in the gene encoding the herpes simplex virus type 1 UL37 polypeptide abrogates virus maturation. J. Virol. **75:**10259–10271.

9. **Desai, P. J.** 2000. A null mutation in the UL36 gene of herpes simplex virus type 1 results in accumulation of unenveloped DNA-filled capsids in the cytoplasm of infected cells. J. Virol. **74:**11608–11618.
10. **Donnelly, M., and G. Elliott.** 2001. Fluorescent tagging of herpes simplex virus tegument protein VP13/14 in virus infection. J. Virol. **75:**2575–2583.
11. **Elliott, G., W. Hafezi, A. Whiteley, and E. Bernard.** 2005. Deletion of the VP22-encoding gene (UL49) alters the expression, localization, and virion incorporation of ICP0. J. Virol. **79:**9735–9745.
12. **Elliott, G., G. Mouzakitis, and P. O'Hare.** 1995. VP16 interacts via its activation domain with VP22, a tegument protein of herpes simplex virus, and is relocated to a novel macromolecular assembly in coexpressing cells. J. Virol. **69:**7932–7941.
13. **Elliott, G., and P. O'Hare.** 2000. Cytoplasm-to-nucleus translocation of a herpesvirus tegument protein during cell division. J. Virol. **74:**2131–2141.
14. **Elliott, G., and P. O'Hare.** 1998. Herpes simplex virus type 1 tegument protein VP22 induces the stabilization and hyperacetylation of microtubules. J. Virol. **72:**6448–6455.
15. **Elliott, G., and P. O'Hare.** 1999. Live-cell analysis of a green fluorescent protein-tagged herpes simplex virus infection. J. Virol. **73:**4110–4119.
16. **Fuchs, W., H. Granzow, B. G. Klupp, M. Kopp, and T. C. Mettenleiter.** 2002. The UL48 tegument protein of pseudorabies virus is critical for intracytoplasmic assembly of infectious virions. J. Virol. **76:**6729–6742.
17. **Fuchs, W., H. Granzow, and T. C. Mettenleiter.** 2003. A pseudorabies virus recombinant simultaneously lacking the major tegument proteins encoded by the UL46, UL47, UL48, and UL49 genes is viable in cultured cells. J. Virol. **77:**12891–12900.
18. **Fuchs, W., B. G. Klupp, H. Granzow, C. Hengartner, A. Brack, A. Mundt, L. W. Enquist, and T. C. Mettenleiter.** 2002. Physical interaction between envelope glycoproteins E and M of pseudorabies virus and the major tegument protein UL49. J. Virol. **76:**8208–8217.
19. **Gross, S. T., C. A. Harley, and D. W. Wilson.** 2003. The cytoplasmic tail of herpes simplex virus glycoprotein H binds to the tegument protein VP16 in vitro and in vivo. Virology **317:**1–12.
20. **Harley, C. A., A. Dasgupta, and D. W. Wilson.** 2001. Characterization of herpes simplex virus-containing organelles by subcellular fractionation: role for organelle acidification in assembly of infectious particles. J. Virol. **75:**1236–1251.
21. **Hutchinson, I., A. Whiteley, H. Browne, and G. Elliott.** 2002. Sequential localization of two herpes simplex virus tegument proteins to punctate nuclear dots adjacent to ICP0 domains. J. Virol. **76:**10365–10373.
22. **Kopp, M., B. G. Klupp, H. Granzow, W. Fuchs, and T. C. Mettenleiter.** 2002. Identification and characterization of the pseudorabies virus tegument proteins UL46 and UL47: role for UL47 in virion morphogenesis in the cytoplasm. J. Virol. **76:**8820–8833.
23. **La Boissiere, S., A. Izeta, S. Malcomber, and P. O'Hare.** 2004. Compartmentalization of VP16 in cells infected with recombinant herpes simplex virus expressing VP16-green fluorescent protein fusion proteins. J. Virol. **78:**8002–8014.
24. **Leslie, J., F. J. Rixon, and J. McLauchlan.** 1996. Overexpression of the herpes simplex virus type 1 tegument protein VP22 increases its incorporation into virus particles. Virology **220:**60–68.
25. **Martin, A., P. O'Hare, J. McLauchlan, and G. Elliott.** 2002. The herpes simplex virus tegument protein VP22 contains overlapping domains for cytoplasmic localization, microtubule interaction, and chromatin binding. J. Virol. **76:**4961–4970.
26. **Mettenleiter, T. C.** 2002. Herpesvirus assembly and egress. J. Virol. **76:**1537–1547.
27. **Miranda-Saksena, M., P. Armati, R. A. Boadle, D. J. Holland, and A. L. Cunningham.** 2000. Anterograde transport of herpes simplex virus type 1 in cultured, dissociated human and rat dorsal root ganglion neurons. J. Virol. **74:**1827–1839.
28. **Penfold, M. E., P. Armati, and A. L. Cunningham.** 1994. Axonal transport of herpes simplex virions to epidermal cells: evidence for a specialized mode of virus transport and assembly. Proc. Natl. Acad. Sci. USA **91:**6529–6533.
29. **Pomeranz, L. E., and J. A. Blaho.** 2000. Assembly of infectious herpes simplex virus type 1 virions in the absence of full-length VP22. J. Virol. **74:**10041–10054.
30. **Pomeranz, L. E., and J. A. Blaho.** 1999. Modified VP22 localizes to the cell nucleus during synchronized herpes simplex virus type 1 infection. J. Virol. **73:**6769–6781.
31. **Read, G. S., B. M. Karr, and K. Knight.** 1993. Isolation of a herpes simplex virus type 1 mutant with a deletion in the virion host shutoff gene and identification of multiple forms of the *vhs* (UL41) polypeptide. J. Virol. **67:**7149–7160.
32. **Rixon, F.** 1993. Structure and assembly of herpesviruses. Semin. Virol. **4:**135–144.
33. **Roizman, B., and A. E. Sears.** 1991. Herpes simplex viruses and their replication, p. 849–895. *In* B. N. Fields and D. M. Knipe (ed.), Fundamental virology. Raven Press, New York, N.Y.
34. **Smibert, C. A., B. Popova, P. Xiao, J. P. Capone, and J. R. Smiley.** 1994. Herpes simplex virus VP16 forms a complex with the virion host shutoff protein vhs. J. Virol. **68:**2339–2346.
35. **Weinheimer, S. P., B. A. Boyd, S. K. Durham, J. L. Resnick, and D. R. O'Boyle, 2nd.** 1992. Deletion of the VP16 open reading frame of herpes simplex virus type 1. J. Virol. **66:**258–269.
36. **Willard, M.** 2002. Rapid directional translocations in virus replication. J. Virol. **76:**5220–5232.
37. **Zhang, Y., D. A. Sirko, and J. L. McKnight.** 1991. Role of herpes simplex virus type 1 UL46 and UL47 in alpha TIF-mediated transcriptional induction: characterization of three viral deletion mutants. J. Virol. **65:**829–841.